



Thermal ablation of ultrasound and non-contrast computed tomography invisible primary and secondary liver tumors: targeting by selective intra-arterial lipiodol injection

Adrian Kobe 
 Lambros Tselikas 
 Frédéric Deschamps 
 Charles Roux 
 Alexandre Delpla 
 Eloi Varin 
 Antoine Hakime 
 Thierry de Baère 

PURPOSE

To evaluate the technical feasibility and outcomes of thermal ablation following selective intra-arterial lipiodol injection (SIALI) for targeting primary and secondary liver tumors invisible on ultrasound (US) and non-contrast computed tomography (CT).

METHODS

This retrospective study included 18 patients with 20 tumors (67% male, mean age 60.8 ± 12.1 years). The 20 tumors included 15 liver metastases and 5 hepatocellular carcinomas. All patients underwent single-session SIALI and subsequent CT-guided thermal ablation. The primary outcome was a technical success, defined as visualization of the tumor after SIALI and successful thermal ablation. Secondary outcomes were local recurrence rate and procedure-related complications.

RESULTS


The median tumor size was 1.5 (1–2.5) cm. In addition, SIALI was performed with a median volume of 3 (1–10) mL of lipiodol resulting in intra-tumoral iodized oil accumulation in 19 tumors and negative imprint with iodized oil accumulation of the surrounding liver parenchyma in 1 tumor. The technical success rate was 100%. No local occurrence was observed at a mean follow-up time of 3 ± 2.5 years.

CONCLUSION

SIALI to tag liver tumors not visible with US and non-contrast CT before percutaneous ablation is highly feasible and has a high success rate for the treatment of both primary and secondary liver tumors.

KEYWORDS

HCC, invisible tumor, liver metastases, selective intra-arterial lipiodol injection, thermal ablation

From the Department of Interventional Radiology, (A.K.,  adrian.kobe@gustaveroussy.fr, L.T., F.D., C.R., A.D., E.V., A.H., T.de B.), Gustave Roussy-Cancer Center, Villejuif, France.

Received 16 January 2022; revision requested 26 January 2022; last revision received 14 March 2022; accepted 04 April 2022.



Epub: 28.12.2022

Publication date: 21.07.2023

DOI: 10.4274/dir.2022.221317

Percutaneous thermal ablation of primary and secondary liver tumors is an accepted alternative to surgery for tumors measuring less than 3 cm.¹⁻³ Thermal ablation is typically guided by ultrasound (US) or non-contrast computed tomography (CT).¹ However, in some cases, the lesions are not visible on either imaging method. Different techniques, such as image fusion with pre-treatment magnetic resonance imaging (MRI) or pre-treatment perilesional coil placement, have been utilized to overcome this problem.^{4,5} Another promising technique is CT-guided thermal ablation after selective intra-arterial lipiodol injection (SIALI) with accumulation in the target tumor, mostly used today for hepatocellular carcinomas (HCCs).^{6,7} So far, no studies exist that evaluate the efficacy of SIALI and subsequent thermal ablation in secondary liver tumors.

Hence, this study aims to evaluate thermal ablation's feasibility and therapeutic outcomes following SIALI for targeting US- and non-contrast-CT-invisible, mostly secondary, liver tumors.

You may cite this article as: Kobe A, Tselikas L, Deschamps F, et al. Thermal ablation of ultrasound and non-contrast computed tomography invisible primary and secondary liver tumors: targeting by selective intra-arterial lipiodol injection. *Diagn Interv Radiol.* 2023;29(4):609-613.

Methods

This retrospective study was approved by the institutional review board (protocol number 2022-111). Written informed consent was waived.

Patients

Between April 2003 and January 2021, 103 patients underwent a single-session combined treatment of SIALI (or lipiodol-based transarterial chemoembolization) and percutaneous thermal ablation in various organs (Figure 1). Among the 84 patients treated with SIALI in the liver, 66 were treated in combination with chemotherapy for liver tumors of 3–5 cm with the goal of improving local tumor control with ablation.⁸ The final study cohort consisted of 18 patients with 20 liver lesions, smaller than 3 cm and invisible on US and non-contrast CT (66.7% male, mean age 60.8 ± 12.1 years), treated with SIALI for the purpose of tumor visualization and thermal ablation.

Baseline characteristics are reported in Table 1. All patients had MRI or multiphase CT scans (native, arterial, portal venous, and delayed phase) of the liver at baseline, with the liver lesions only visible on the arterial phases. Five lesions were HCCs (25%), whereas the other 15 lesions were liver metastases from various locations (75%) (Table 1).

Interventional techniques

All interventions took place under general anesthesia in a hybrid room made of an angiography system (angioCT alphenix 4D+, Canon Medical Systems, Otawara, Japan) and a multidetector CT (MDCT) (Acquillion one Genesis, Canon Medical Systems, Otawara, Japan; LightSpeed 16, GE Medical Systems, Milwaukee, WI, USA).

SIALI

After the puncture of the common right femoral artery, a 5F sheath was inserted,

Main points

- Treatment of small liver tumors by percutaneous thermal ablation that are invisible on ultrasound or non-contrast computed tomography is challenging.
- Primary and secondary liver tumors can be visualized by selective intra-arterial lipiodol injection (SIALI), enabling same-session percutaneous thermal ablation.
- SIALI proved feasible with excellent oncologic outcomes and allowed for the treatment of both primary and secondary liver tumors.

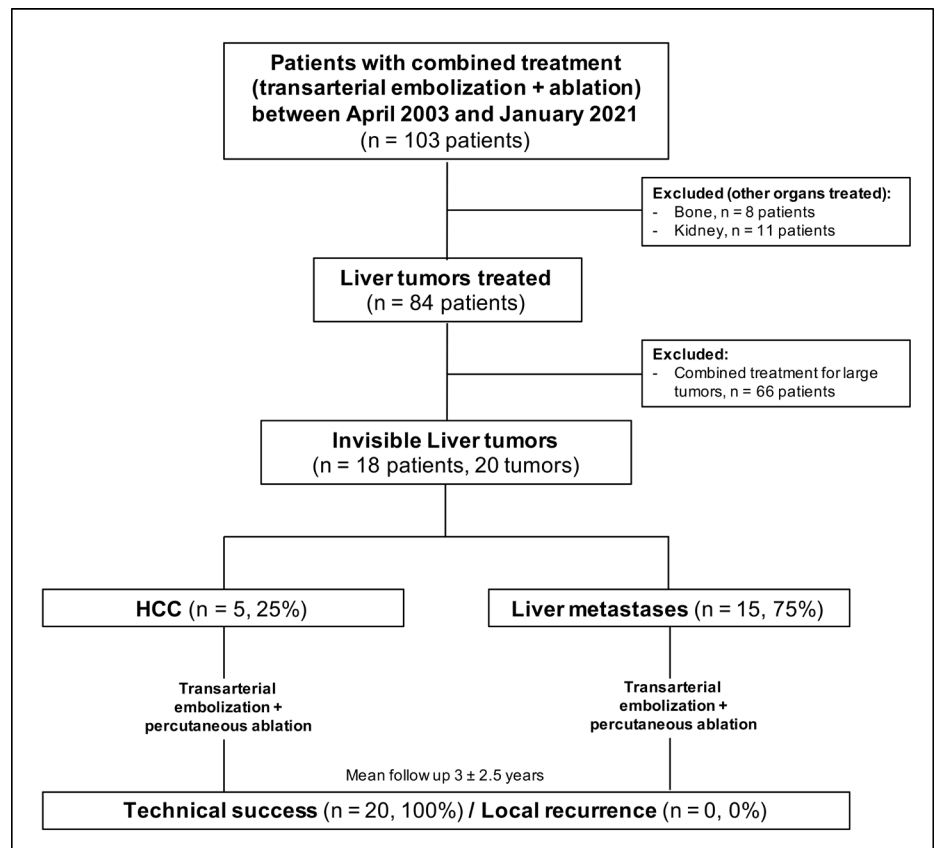


Figure 1. Patient inclusion and outcome flowchart. HCC, hepatocellular carcinoma.

Table 1. Baseline patient characteristics

	All
Total patients, n (%)	18 (100)
Age (years), mean ± SD	60.8 ± 12.1
Male, n (%)	12 (66.7)
Encountered histology	
Number of tumors treated, n (%)	20 (100)
HCC, n (%)	5 (25)
Metastases, n (%)	15 (75)
Neuroendocrine, n (%)	11 (73.3)
Adrenal carcinoma, n (%)	1 (6.7)
Thyroid carcinoma, n (%)	1 (6.7)
Paraganglioma, n (%)	1 (6.7)
GIST, n (%)	1 (6.7)
Tumor specifications	
Tumor size (cm), median (min–max)	1.5 (1–2.5)
Previous treatments	
No, n (%)	2 (11.1)
Surgery, n (%)	12 (66.7)
Radiotherapy, n (%)	1 (5.6)
IR, n (%)	8 (44.4)
Systemic chemotherapy, n (%)	8 (44.4)
Liver segment	
II	2 (10)
IV	3 (15)
V	1 (5)
VI	7 (35)
VII	2 (10)
VIII	5 (25)

GIST, gastrointestinal stromal tumor; HCC, hepatocellular carcinoma; IR, Interventional Radiology; SD, standard deviation.

and the common hepatic artery was catheterized. A digital subtraction angiography was performed to detect all tumor feeders. In case tumor feeders were not detected on digital subtraction angiography, a CT angiography was also carried out to locate the tumor-feeding arteries. Next, selective catheterization of the corresponding vessel was performed using a 2.4F microcatheter (PROGREAT®, Terumo, Tokyo, Japan). A CT angiography was conducted over the placed microcatheter to verify that the entirety of the tumor was covered. Iodized oil (Lipiodol Ultrafluid, Guerbet, Aulnay-Sons-Bois, France) emulsified with saline in a 3:1 ratio was injected into the corresponding artery. The SIALI endpoint was the visualization of the tumor on non-contrast CT.

Percutaneous ablation

Percutaneous ablation was performed immediately after SIALI once tumor tagging was confirmed on MDCT. A thermal ablation probe was inserted into the tumor under real-time MDCT guidance. The liver tumors were either treated by radiofrequency ablation (RFA), microwave ablation (MWA), or cryoablation (CRA) based on the preference of the treating interventional radiologist.

For RFA, either a deployable RFA needle (LeVein, Boston Scientific, Natick, MA, USA) (Figure 2) or a triple cluster probe (Cool-tip™ RFA Cluster Electrode 2.5 cm active tip, Covidien, Mansfield, MA, USA) (Figure 3) was used. The standard ablation protocol consisted of 12 min with a target final temperature of 60°C or above for the triple cluster probe. For the deployable RFA needle, the ablation session was started at an energy of 30 W and increased by 10 W every 60 s until tissue impedance was raised and a roll-off was reached. In case the roll-off was reached before 12 min, an additional ablation session was performed.

The MWA was performed with microwave probes from different vendors. The time and power of ablation were adapted according to the tumor size, location, and comprehensive protocols supplied by the generator supplier.

The CRA was performed with a cryo-system (VISUAL ICE™, Boston Scientific, Natick, MA, USA) and multiple cryoprobes (IceSphere™ or IceRod™) to cover the entire lesion. A standard treatment cycle consisted of two freeze cycles over 10 min with an intermittent 10 min thawing cycle (9 min passive heating, 1 min active heating).

A safety margin of 5 mm between the SIALI visualized tumor and the ablation zone, monitored with periprocedural CT, was considered sufficient for thermal ablation.

Follow-up treatment

Follow-up treatment consisted of clinical visits and imaging at 1, 2, 6, and 12 months, with subsequent annual visits. Technical success was defined as the visualization of the tumor after SIALI and successful thermal ablation. Local recurrence was defined as any contrast-enhancing nodular lesion in the treated area evaluated by multiphase CT or contrast-enhanced MRI. Complications were classified according to the Society of Interventional Radiology (SIR) standards of practice committee with a SIR adverse event (AE) severity scale of 1 to 5.⁹ The primary outcome was a technical success. Secondary outcomes were local recurrence and procedure-related complications.

Statistical analysis

The Shapiro–Wilk test was used to test for the normal distribution of data. For descriptive data, mean values and standard deviations, as well as median (min–max) values, were provided as appropriate. Categorical variables were reported as frequencies and percentages. IBM SPSS software v25.0 was used for data analysis.

Results

Median tumor size was 1.5 (1–2.5) cm with 5 HCCs (25%) and 15 liver metastases (75%) treated. After SIALI with a median volume of 3 (1–10) mL of iodized oil, all but one tumor (95%) showed intra-tumoral iodized oil accumulation with enough conspicuity for ablation targeting. In one patient (5%), the tumor was visualized by a negative imprint with lipiodol accumulation of the surrounding liver parenchyma (Figure 4).

Thermal ablation was performed using a cluster probe RFA in seven cases (39%) with a mean ablation time of 11.6 ± 4 min and a mean end temperature of $79^\circ\text{C} \pm 6.4^\circ\text{C}$. A deployable RFA needle was used in four cases (22%), and MWA was used in six cases (33%) with a mean applied power of 84 ± 22 W and a mean ablation time of 10 ± 3.5 min. CRA was used in one case (6%).

One complication (5.6%) was encountered (SIR AE severity scale 4) with cardiac arrest due to hormone discharge during ablation of a paraganglioma metastasis. In-hospital mortality was 0%. The first follow-up CT demonstrated ablation zones measuring $4 \pm$

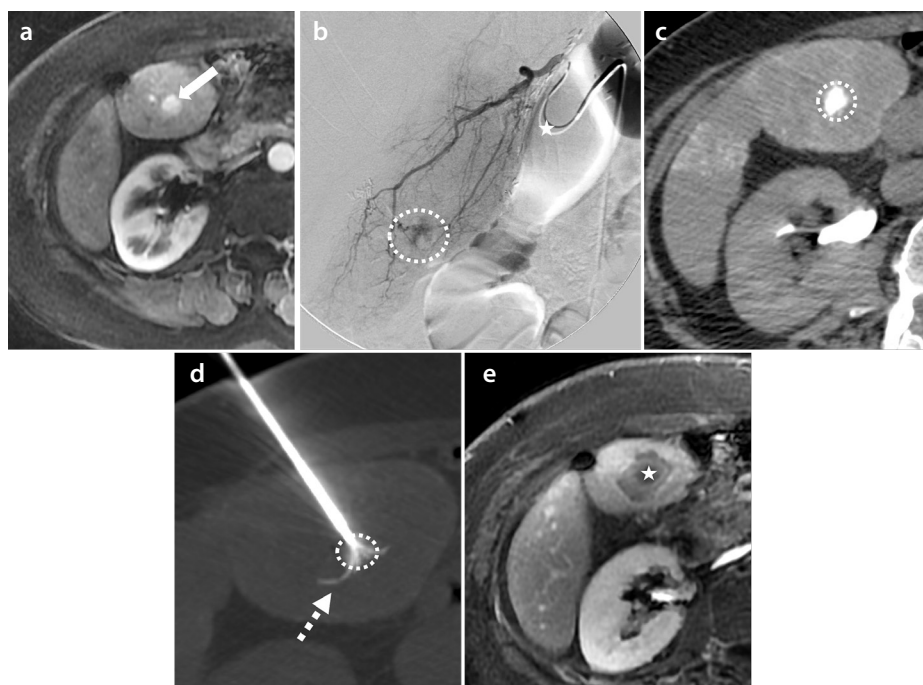


Figure 2. Tagging of a liver metastasis from a neuroendocrine tumor by selective intra-arterial iodized oil injection and subsequent radiofrequency ablation (RFA) in a 56-year-old female. Panel (a) shows an arterial phase of the pre-treatment magnetic resonance imaging (MRI) with a hypervascular tumor measuring 12 mm in segment IVb (white arrow). Panel (b) shows the selective angiography with a microcatheter (white star) placed in the segment IVa artery and a tumor blush (dotted circle). After injection of 2 mL of iodized oil, the tumor showed strong accumulation [dotted circle panel (c)]. Subsequently, an expandable RFA needle (LeVein, Boston Scientific, Natick, MA, USA) (dotted white arrows) was placed under computed tomography guidance covering the entire tumor [panel (d)]. Panel (e) shows a contrast-enhanced MRI six months after treatment without evidence of tumor recurrence (white star).



Figure 3. Tagging of a hepatocellular carcinoma by selective intra-arterial iodized oil injection and subsequent radiofrequency ablation (RFA) in a 54-year-old male. Panel (a) shows an arterial phase of the pre-treatment computed tomography (CT) with a hypervascular tumor measuring 14 mm in segment VIII (white arrow). Panel (b) shows the selective angiography with a microcatheter (white star) placed in the segment VIII artery and a tumor blush (dotted circle). After the injection of 3 mL of iodized oil, the tumor showed moderate accumulation [dotted circle panel (c)]. Subsequently, a triple cluster probe (Cool-tip™ RFA Cluster Electrode 2.5 cm active tip, Covidien, Mansfield, MA, USA) was placed under CT guidance [panel (d)]. The needle was placed transthoracically and diaphragmatically after creating an iatrogenic pneumothorax. Panel (e) shows a contrast-enhanced CT six months after treatment without evidence of tumor recurrence and the ablation zone (white dotted arrows) covering the entire tumor.

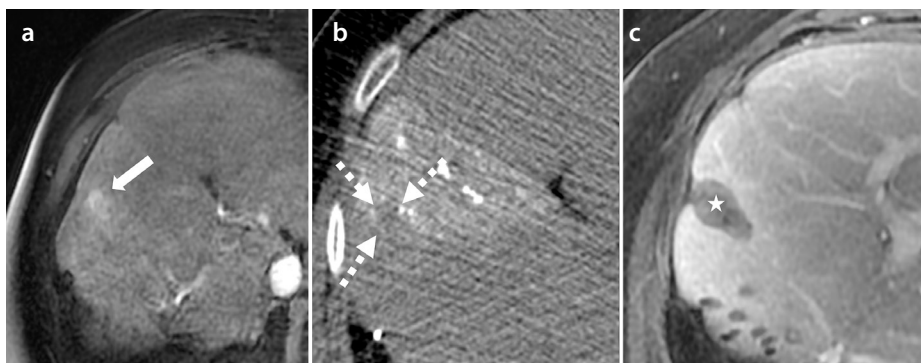


Figure 4. Tagging of a liver metastasis from a neuroendocrine tumor by selective intra-arterial iodized oil injection and subsequent microwave ablation in a 46-year-old male. Panel (a) shows an arterial phase of the pre-treatment magnetic resonance imaging (MRI) with a hypervascular tumor measuring 14 mm in segment IV (white arrow). The selective angiography of the segment IV artery did not reveal any tumoral blush. However, a total of 2 mL of iodized oil was injected with accumulation in the peritumoral liver parenchyma, enabling the detection of the tumor (white dotted arrows) on non-contrast intraprocedural computed tomography [panel (b)]. Subsequently, microwave ablation was performed without evidence of tumor recurrence (white star) on a follow-up MRI at six months [Panel (c)].

1.2 cm, which completely encompassed the targeted tumors with safety margins. The tumors were still visible at the time of follow-up due to iodized oil retention.

No local recurrence was observed during a mean follow-up period of 3 ± 2.5 years. Distant progression was observed in 11 patients

(61.1%), with a mean time to systemic progression of 2.1 ± 1.5 years. Table 2 summarizes all intervention-related characteristics.

Discussion

The present study indicates that targeting invisible liver metastases by SIALI immedi-

ately before percutaneous ablation is highly feasible with a high local tumor control rate, as it is for primary liver tumors.

For percutaneous ablation, the visibility of the target lesion is of utmost importance, and US or non-contrast CT guidance is most commonly used. In tumors not depicted with US or non-contrast CT guidance, the technique to tag liver tumors by SIALI described in this study carries multiple advantages. First, it is a low-cost, ubiquitous technology with low additional intervention-related risks. Second, no additional software or hardware is needed. However, when MDCT and angiography are not located in the same room, either the puncture can be obtained under cone beam computed tomography (CBCT) guidance, or the patient has to be moved from the angiography suite to the MDCT after SIALI.^{10,11} Even if there is a personal experience with CBCT-guided puncture after SIALI not reported here, the optimal solution is certainly an integrated angiography-CT suite, which is increasingly common in interventional oncology departments.¹²

An alternative technique for targeting US and CT non-visible lesions is image fusion with pre-treatment contrast-enhanced images, where the tumor is visualized.¹³ However, image fusion has limitations due to different breathing phases and arm positioning between pre-treatment and per-treatment imaging, causing differences in liver configuration.¹⁴ This problem might be overcome by non-rigid image registration, which is technically more demanding and likely unavailable today in routine practice.¹⁵ Furthermore, due to diaphragm motion during breathing, tumors located in the hepatic dome are highly challenging. Especially in the case of special percutaneous access routes, such as a transthoracic/diaphragmatic probe placement after creating an artificial pneumothorax (Figure 3), image fusion is limited due to major hepatic deformations. Other emerging fields trying to solve the difficulties of invisible targets are stereotactic image-guided navigation and robotic navigation systems with trajectory planning on contrast-enhanced CT scans obtained before treatment.^{13,16} However, these systems are associated with very high costs and low availability.

There are few studies in the literature examining the feasibility and long-term outcomes of SIALI or lipiodol-based transarterial chemoembolization for targeting small invisible HCCs, reporting excellent tumor visualization and local tumor control rates of 90%–100%.^{6,7,17–20} While no published data exists for secondary liver tumors, the current cohort demonstrates successful tagging of

Table 2. Treatment and follow-up characteristics

	All
Intervention	
Type of ablation	
RFA cluster, n (%)	7 (38.9)
RFA expandable, n (%)	4 (22.2)
Ablation time (min), mean ± SD	11.6 ± 4
End temperature (°C), mean ± SD	79 ± 6.4
Microwave ablation, n (%)	6 (33.3)
Cryoablation, n (%)	1 (5.6)
Type of embolization	
Lipiodol	20 (100)
Lipiodol volume (mL), median (min–max)	3 (1–10)
Lipiodol retention, n (%)	19 (95)
Organ at risk in vicinity, n (%)	3 (16.7)
Technical success, n (%)	20 (100)
Ablation zone, mean ± SD	4 ± 1.2
In-hospital outcome	
Complications, n (%)	1 (5.6)
In-hospital mortality, n (%)	0 (0)
Hospital stay (days), median (min–max)	3 (1–8)
Follow-up (years), mean ± SD	
Local recurrence, n (%)	0 (0)
Systemic progression, n (%)	11 (61.1)
Time to systemic progression (years), mean ± SD	2.1 ± 1.5
RFA, Radiofrequency ablation; SD, Standard deviation.	

all 15 secondary liver tumors from various primary origins, mostly with intratumoral lipiodol accumulation but also with negative staining due to iodized oil accumulation in the surrounding liver parenchyma (Figure 4). The 100% local tumor control rate after a mean follow-up period of 3 ± 2.5 years demonstrates the high effectiveness of SIALI, which is related to the precise needle positioning during percutaneous thermal ablation.

The main limitations of this study are the retrospective design and the limited number of patients.

In conclusion, utilizing SIALI to tag US- and non-contrast-CT-invisible liver tumors for percutaneous ablation is feasible with excellent outcomes and allows for the treatment of both primary and secondary liver tumors.

Conflict of interest disclosure

The authors declared no conflicts of interest.

References

1. Crocetti L, de Baère T, Pereira PL, Tarantino FP. CIRSE standards of practice on thermal ablation of liver tumours. *Cardiovasc Intervent Radiol.* 2020;43(7):951–962. [\[CrossRef\]](#)
2. Van Cutsem E, Cervantes A, Adam R, et al. ESMO consensus guidelines for the management of patients with metastatic colorectal cancer. *Ann Oncol.* 2016;27(8):1386–1422. [\[CrossRef\]](#)
3. Vogel A, Cervantes A, Chau I, et al. Hepatocellular carcinoma: ESMO Clinical

Practice Guidelines for diagnosis, treatment and follow-up. *Ann Oncol.* 2018;29(Suppl 4):iv238–iv255. Erratum for: *Ann Oncol.* 2018 Oct 1;29(Suppl 4):iv238–iv255. [\[CrossRef\]](#)

4. Schullian P, Johnston E, Laimer G, et al. Thermal ablation of CT 'invisible' liver tumors using MRI fusion: a case control study. *Int J Hyperther.* 2020;37(1):564–572. [\[CrossRef\]](#)
5. Adam A, Hatzidakis A, Hamady M, Sabharwal T, Gangi A. Percutaneous coil placement prior to radiofrequency ablation of poorly visible hepatic tumors. *Eur Radiol.* 2004;14(9):1688–1691. [\[CrossRef\]](#)
6. Nakajima K, Yamanaka T, Nakatsuka A, et al. Clinical utility of radiofrequency ablation following transarterial injection of miriplatin-iodized oil suspension in small hepatocellular carcinoma. *Jpn J Radiol.* 2016;34(9):640–646. [\[CrossRef\]](#)
7. Takaki H, Yamakado K, Nakatsuka A, et al. Computed tomography fluoroscopy-guided radiofrequency ablation following intra-arterial iodized-oil injection for hepatocellular carcinomas invisible on ultrasonographic images. *Int J Clin Oncol.* 2013;18(1):46–53. [\[CrossRef\]](#)
8. Chu HH, Kim JH, Yoon HK, et al. Chemoembolization combined with radiofrequency ablation for medium-sized hepatocellular carcinoma: a propensity-score analysis. *J Vasc Interv Radiol.* 2019;30(10):1533–1543. [\[CrossRef\]](#)
9. Khalilzadeh O, Baerlocher MO, Shyn PB, et al. Proposal of a New Adverse Event Classification by the Society of Interventional Radiology Standards of Practice Committee. *J Vasc Interv Radiol.* 2017;28(10):1432–1437.e3. [\[CrossRef\]](#)

10. Lyu T, Wang J, Cao S, Song L, Tong X, Zou Y. Radiofrequency ablation guided by cone beam computed tomography for hepatocellular carcinoma: a comparative study of clinical results with the conventional spiral computed tomography-guided procedure. *J Int Med Res.* 2019;47(8):3699–3708. [\[CrossRef\]](#)
11. Bapst B, Lagadec M, Breguet R, Vilgrain V, Ronot M. Cone Beam Computed Tomography (CBCT) in the field of interventional oncology of the liver. *Cardiovasc Intervent Radiol.* 2016;39(1):8–20. Erratum in: *Cardiovasc Intervent Radiol.* 2015;38(5):1381. [\[CrossRef\]](#)
12. Erinjeri JP, Doustaly R, Avignon G, et al. Utilization of integrated angiography-CT interventional radiology suites at a tertiary cancer center. *Bmc Med Imaging.* 2020;20(1):114. [\[CrossRef\]](#)
13. Hui TC, Kwan J, Pua U. Advanced techniques in the percutaneous ablation of liver tumours. *Diagnostics (Basel).* 2021;11(4):585. [\[CrossRef\]](#)
14. Kobe A, Kindler Y, Klotz E, et al. Fusion of preinterventional MR imaging with liver perfusion CT After RFA of hepatocellular carcinoma: early quantitative prediction of local recurrence. *Invest Radiol.* 2020;56(3):188–196. [\[CrossRef\]](#)
15. Park J, Lee J, Lee D, et al. Value of Nonrigid Registration of Pre-Procedure MR with Post-Procedure CT after radiofrequency ablation for hepatocellular carcinoma. *Cardiovasc Intervent Radiol.* 2017;40(6):873–883. [\[CrossRef\]](#)
16. Guiu B, De Baère T, Noel G, Ronot M. Feasibility, safety and accuracy of a CT-guided robotic assistance for percutaneous needle placement in a swine liver model. *Sci Rep.* 2021;11(1):5218. Erratum in: *Sci Rep.* 2021;11(1):8241. [\[CrossRef\]](#)
17. Gandhi S, Iannitti DA, Mayo-Smith WW, Dupuy DE. Technical report: lipiodol-guided computed tomography for radiofrequency ablation of hepatocellular carcinoma. *Clin Radiol.* 2006;61(10):888–891. [\[CrossRef\]](#)
18. Lee MW, Kim YJ, Park SW, et al. Percutaneous radiofrequency ablation of small hepatocellular carcinoma invisible on both ultrasonography and unenhanced CT: a preliminary study of combined treatment with transarterial chemoembolisation. *Br J Radiology.* 2009;82(983):908–915. [\[CrossRef\]](#)
19. Hyun D, Cho SK, Shin SW, Rhim H, Koh KC, Paik SW. Treatment of small hepatocellular carcinoma (≤ 2 cm) in the caudate lobe with sequential transcatheter arterial chemoembolization and radiofrequency ablation. *Cardiovasc Intervent Radiol.* 2016;39(7):1015–1022. [\[CrossRef\]](#)
20. Pan F, Do TD, Vollherbst DF, et al. Percutaneous irreversible electroporation for treatment of small hepatocellular carcinoma invisible on unenhanced CT: a novel combined strategy with prior transarterial tumor marking. *Cancers.* 2021;13(9):2021. [\[CrossRef\]](#)